5th ECPMG Delft · 2024

Proceedings of the 5th ECPMG 2024
5th European Conference on Physical Modelling in Geotechnics
2-4 October 2024, Delft, the Netherlands

Centrifuge model tests on liquefaction countermeasure for road bridge pile foundations in volcanic ash ground

T. Egawa, H. Hayashi
Civil Engineering Research Institute for Cold Region, Sapporo, Japan, egawa@ceri.go.jp, hayashi@ceri.go.jp
K. Isobe
Hokkaido University, Sapporo, Japan, kisobe@eng.hokudai.ac.jp

ABSTRACT: This study explores seismic reinforcement techniques for road bridge pile foundations in volcanic ash ground. The proposed method involves encircling the pile foundation with a grid-form ground improvement wall for liquefaction countermeasures without direct contact with existing structures. Centrifuge model tests on commonly used road bridge pile foundations assessed the effects of different spacings and improvement strengths of the grid-form ground improvement wall on liquefaction countermeasure efficiency and the impact on existing piles. Results indicate that, irrespective of pile type or stiffness, the proposed technique had no significant impact on existing bridge superstructures. A recommended grid spacing of 7.0m or less, with an outermost pile center distance of 2.0m or more, was identified as suitable for achieving non-invasive reinforcement and effective counteraction of the reduction in horizontal subgrade reaction coefficients due to liquefaction, with sufficient performance achieved by adjusting the improvement strength and layout within this range.

1 INTRODUCTION

In Japan, efforts are underway to implement seismic measures for existing road bridges in anticipation of major earthquakes. Some older pile foundations of road bridges, predating the current seismic standards, fall short of compliance. While certain pile foundations necessitate enhanced structural rigidity, others can meet current seismic standards by solely addressing liquefaction in the adjacent ground. This holds true for pile foundations in volcanic coarse-grained soils, prevalent in Hokkaido and Kyushu, recognized as problematic soils in Japan. It is necessary to enhance the menu of reinforcement methods that address various factors contributing to inadequate seismic performance and on-site construction conditions.

In light of the above, we have been exploring the viability of a ground improvement technique utilizing grid-form walls. These walls encompass the ground around the pile foundation without direct contact with the existing structure, serving as a seismic reinforcement method when the stability of pile foundations is jeopardized solely by liquefaction in volcanic ash ground.

In this study, centrifuge model tests were conducted to assess how grid-form ground improvement walls impact liquefaction mitigation and the stability of existing pile foundations. We varied the strength and separation of the improvement walls from the outermost piles. The experimental focus involved steel pipe piles (SPPs) and cast-in-place concrete piles (CCPs), commonly employed in road bridge foundations.

2 OUTLINE OF THE CENTRIFUGE MODEL TEST

Figure 1 shows schematics of the experimental model SPP4*D*-1000. Figure 2 shows schematics of the experimental model CCP2*D*-300.

The centrifuge model tests consisted of static horizontal loading tests followed by dynamic vibration tests. In both tests, a centrifugal acceleration of 50*g* was applied to the experimental cases shown in Table 1 (SPPs) and Table 2 (CCPs). The static horizontal loading tests were conducted such as to achieve a horizontal displacement of the piles at the ground surface of 1% or more than the pile diameter, with no residual displacement remaining in the pile or the surrounding ground. For the dynamic vibration test, one vibration was performed with the sinusoidal wave shown in the table.

The model piles were arranged as a set of four piles (2×2) with a pile center-to-center spacing of 3*D* (*D*:pile diameter) for each pile type. Strain gauges were attached to one of the four piles at 11 depths (two gauges per depth).

For the model SPPs, steel pipes with a diameter *D*=10mm and a wall thickness *t*=0.2mm were used. For many national road bridges in Hokkaido, which is widely distributed with volcanic ash ground, SPPs with *D*≅600mm (bending stiffness

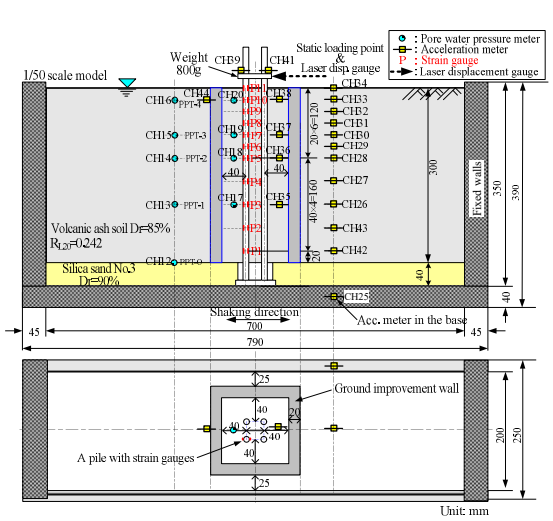

Figure 1. Outline of the experiment model (SPP4D-1000)

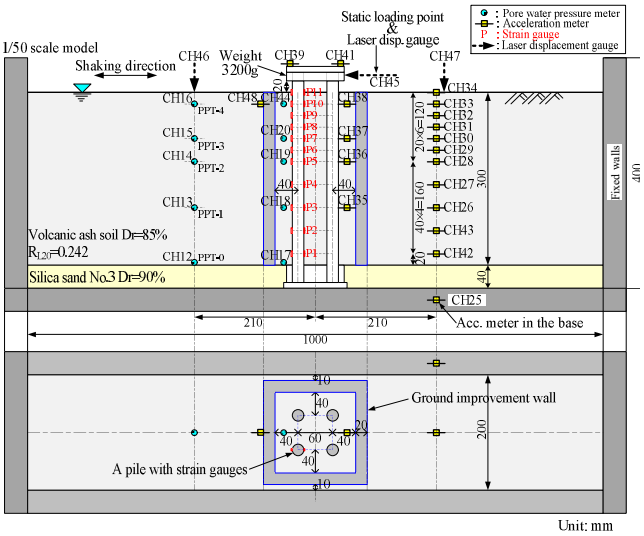

Figure 2. Outline of the experiment model (CCP2D-300)

Table 1. Experiment cases (SPPs)

SPP (D:500mm) Case	Model ground	Ground improvement wall			Input seismic motion
		Wall thickness	Spacing from the center of the outermost pile	Unconfined compression strength q_u	
Without	Volcanic ash soil D_r = 85% R_{L20} = 0.242 [DA = 5%] Layer thickness 300 mm (15.0 m)	-	-	-	20 sine waves Frequency (1.5 Hz) Max. Acc. (200 cm/s^2) Single excitation
2D-1000		20mm (1.0m)	20mm (1.0m)	1,095kN/m^2 [Age 13 days]	
3D-300			30mm (1.5m)	419kN/m^2 [Age 11 days]	
4D-1000			40mm (2.0m)	1,270kN/m^2 [Age 14 days]	
4D-500				963kN/m^2 [Age 11 days]	
4D-300				345kN/m^2 [Age 11 days]	
6D-1000			60mm (3.0m)	934kN/m^2 [Age 11 days]	

* Case names represent the spacing from piles and target strength of ground improvement wall.
* "Without" is "without the improvement wall." * D: Pile diameter. ( ): Prototype scale.

Table 2. Experiment cases (CCPs)

CCP (D:1000mm) Case	Model ground	Ground improvement wall			Input seismic motion
		Wall thickness	Spacing from the center of the outermost pile	Unconfined compression strength q_u	
Without	Volcanic ash soil D_r = 85% R_{L20} = 0.242 [DA = 5%] Layer thickness 300 mm (15.0 m)	-	-	-	20 sine waves Frequency (1.5 Hz) Max. Acc. (200 cm/s2) Single excitation
2D-300		20mm (1.0m)	40mm (2.0m)	339kN/m^2 [Age 11 days]	
2D-1000				900kN/m^2 [Age 11 days]	
3D-300			60mm (3.0m)	423kN/m^2 [Age 11 days]	

* Case names represent the spacing from piles and target strength of ground improvement wall.
* "Without" is "without the improvement wall." * D: Pile diameter. ( ): Prototype scale.

(EI)=1.037×10^{5}kN·m^2) were used for the pile foundations before the current seismic standards were introduced. For the experiment model, we adopted piles with D=500mm (EI=1.053×10^{5}kN·m^2) to represent the diameter of widely used SPPs and to roughly match the EI of those SPPs. For the model CCPs, aluminum pipes with a diameter D=20mm and a wall thickness t=1.0mm were used. We chose these model CCPs under the assumption that they were equivalent to field-size piles with D=1000mm (EI=1.094×10^{6}kN·m^2). The CCPs with D=1000mm (EI=1.227×10^{6}kN·m^2) were often used in bridge foundations before the current standards.

The separation between the ground improvement wall and the outermost pile was set at least 2D from the center of the outermost pile to avoid contact with the existing footing.

High-early-strength Portland cement was used as the ground improvement material to reduce the curing period. The amount of cement, determined by preliminary mixing tests, was mixed with the model ground material in a vacuum mixer as a slurry with a water-cement ratio of W/C=1.0. The slurry was then poured into a form of a predetermined size and air-cured for two days before being used to make the model. The q_u values shown in Tables 1 and 2 are for test pieces that were air-cured until the day of the experiment. These test pieces were not used in the model but were used to determine whether the target strength was obtained.

For the model ground, we used soil from the Shikotsu pumice-flow deposit Spfl, which was sifted through a 0.85mm sieve and used at a dry density of ρ_d=1.094g/cm^3. The Spfl ground had liquefied in several earthquakes, including the 2018 Hokkaido Eastern Iburi Earthquake. The model soil corresponds to a ground material whose relative density is D_r=85% and whose liquefaction strength ratio is R_{L20}=0.242. The pore fluid in the model ground was 50cSt silicone oil, to satisfy the similarity of the accumulation and dissipation of excess pore water pressure. To saturate the model ground, the prepared model ground was deaerated; then, deaerated silicon oil was slowly introduced from the bottom of the soil tank.

3 EXPERIMENT RESULTS

The values, including the measured values, in the following sections will be expressed as those for the real scale.

3.1 Depth distributions for various measured values in the experiments on SPPs

Figure 3 shows the depth distributions for the maximum values of various measurements inside the ground improvement walls in the SPP dynamic vibration test. These are compared to the values from the experiments on the model without the improvement walls.

The shear strain of the ground is obtained by calculating the shear strain time history between two adjacent depth points based on the acceleration time history for each depth point, plotted as the maximum value midway between each pair of measured depth points. The excess pore water pressure was evaluated at the time when the amplitude of shaking had settled. The bending moment of the pile is obtained by averaging the positive and negative absolute values for each amplitude of the time history, and the maximum values are plotted. The ratio of increase/decrease for the horizontal subgrade reaction coefficient of the pile, k_{hL}/k_{h0}, was set as the ratio of the coefficient of dynamic horizontal subgrade reaction, k_{hL}, during the vibration of each case to the coefficient of static horizontal subgrade reaction, k_{h0}, before the vibration for the model without the improvement walls. For k_{h0} and k_{hL}, we used the values when the pile's horizontal displacement at the ground surface was 1% of the pile diameter. The respective calculation procedures are detailed in Egawa et al. (2018). Here, we compare the values for each case at G.L. -1.0m to -5.0m, where k_{h0} was clearly obtained. The figures of k_{hL}/k_{h0} also show the average values for the above depths.

We will discuss how the improvement measure differed in effectiveness with difference in the separation (Figure 3(a)).

The shear strain in the ground was suppressed more in the case with less separation, except for 3*D*-300, and the difference in suppression was even more at shallower depths.

The generation of excess pore water pressure was suppressed the most for the least separation and the least for the largest separation, except for G.L. -10.0m in 3*D*-300. However, the suppression was low in shallow parts of the ground in all cases. Although shear strain generation was suppressed in 6*D*-1000, excess pore water pressure was generated at depths shallower than G.L. -6.0m. The behavior of 6*D*-1000 at depths shallower than G.L.-6.0m was similar to that for the case without improvement walls. We judged that no liquefaction suppression was observed for the separation of 6*D*.

It can be observed that the bending moment in the piles around the ground's mid-depth was suppressed in the cases of 2*D*-1000 and 4*D*-1000 (with improvement walls) but not in the model without improvement walls. For 3*D*-300 and 6*D*-1000, the bending moment around the mid-depth is comparable to the bending moment in the case without the improvement walls. In the case of 3*D*-300, even though the low strength improvement afforded by the improvement walls was effective in controlling excess pore water pressure, that strength improvement caused bending deformation in the walls, and the walls and the ground inside them vibrated and deformed together, resulting in the generation of a large bending moment.

The average value of k_{hL}/k_{h0} at G.L. -1.0m to -5.0m exceeds 1.0 for 2*D*-1000, indicating that the dynamic horizontal subgrade reaction force is greater than that for the case without the improvement walls before the application of vibration. In the case of 2*D*-1000, structural changes to the entire bridge system may be required to address the excessive stresses acting on each member of the existing overground structure of the bridge, to deal with the stresses that are than those in the case without the improvement walls. The k_{hL} of the case without the improvement walls decreased to about 53% of the pre-vibration k_{h0}. It can be observed that the degree of reduction in the coefficient of horizontal subgrade reaction of the pile due to liquefaction was suppressed by about 30% (a decrease to 87%) in 3*D*-300 and by about 50% (a decrease to 105%) in 4*D*-1000. In 6*D*-1000, the improvement walls were observed to afford no improvement, as k_{hL} for 6*D*-1000 decreased to the same level as that of k_{hL} for the model without the improvement walls. In the seismic performance verification of existing road bridges, there were cases in which the current seismic standards would be satisfied with certain improvements. There are cases in which the current standards could be satisfied by a roughly 30% decrease in the reduction coefficient. The reduction coefficient is a coefficient that is multiplied by the soil parameters of the seismic design when liquefaction is the issue to be considered. In cases where a 30% decrease in the reduction coefficient is the key to the improvement plan, this method can be an effective measure when the appropriate conditions are set.

We will discuss the difference in the effectiveness of the improvement measure based on the difference in the strength of the improved wall (Figure 3(b)).

The generation of ground shear strain was suppressed more in all cases with improvement measures than in the cases without the improvement measure. The degree of suppression did not differ with the difference in improved strength of the walls.

The occurrence of excess pore water pressure was suppressed in cases where the strength of the improvement walls was great. In the case of 4*D*-300, excess pore water pressure was found to occur at

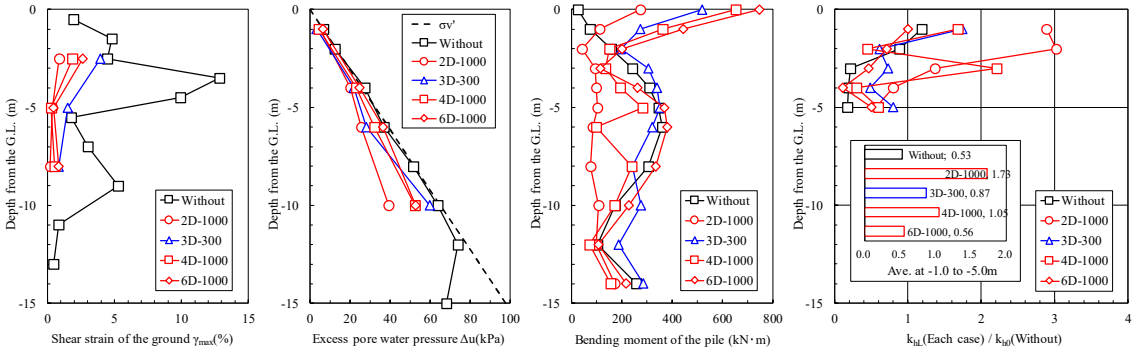

(a) Comparison for different separations.

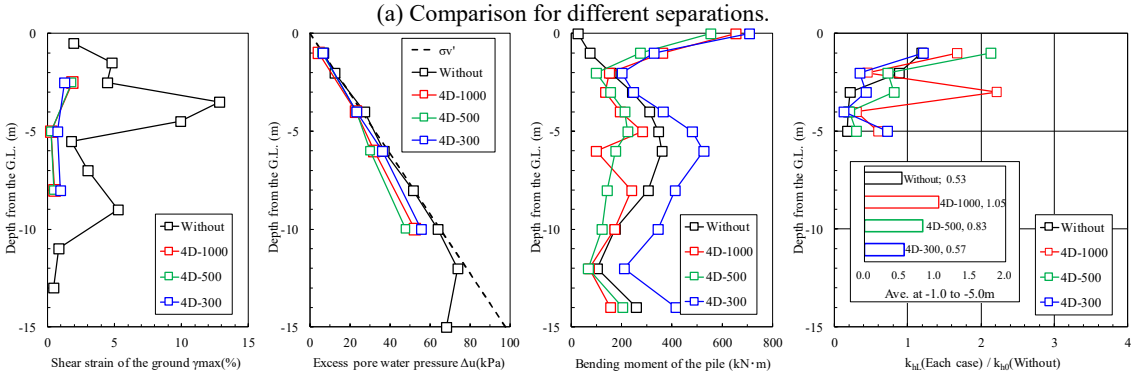

(b) Comparison for different improved strengths.

Figure 3. Depth distribution of various measurement values and k_{hL}/k_{h0} inside the ground improvement wall (SPPs).

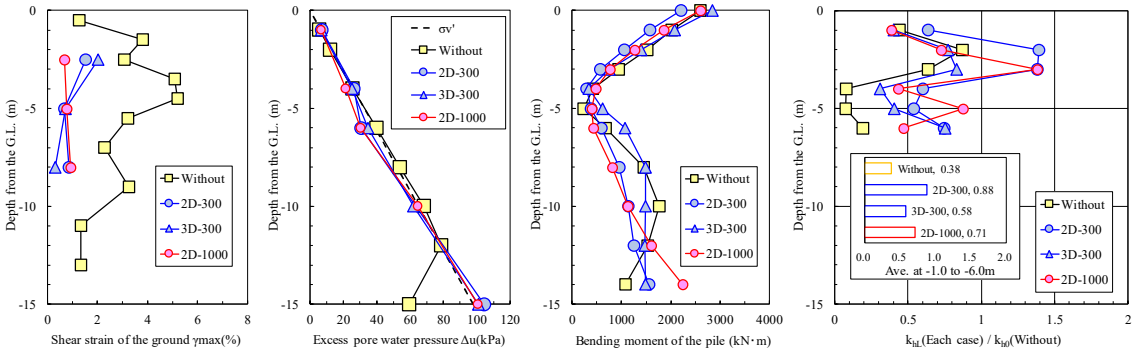

Figure 4. Depth distribution of various measurement values and k_{hL}/k_{h0} inside the ground improvement wall (CCPs).

depths shallower than G.L. -6.0m, as in the case of 6*D*-1000 (Figure 3(a)), which was similar to the occurrence of excess pore water pressure in the model without the improvement measure. It was concluded that 4*D*-300 was ineffective at suppressing liquefaction.

The bending moment of the piles was more suppressed around the mid-depth of the ground in 4*D*-1000 and 4*D*-500 than in the case without the improvement measure, and the values for 4*D*-1000 and 4*D*-500 were generally similar. In the case of 4*D*-300, the bending moment generated in the mid-section of the measured ground was than in the case without the improvement measure. As in the case of 3*D*-300, although the ground improvement walls were not damaged, bending deformation occurred, suggesting that the ground improvement walls vibrated and deformed together with the ground inside the walls.

The average value of k_{hL}/k_{h0} at G.L. -1.0m to -5.0m was 83% for 4*D*-500. The ratio of increase/decrease in the horizontal ground reaction coefficient for 4*D*-500 was suppressed by about 30%, but that for 4*D*-300 decreased to the same level as that of the model without the improvement measure. The measure was recognized as affording no improvement in the case of 4*D*-300.

Although we found no improvement for 4*D*-300, the case of 3*D*-300 showed the suppression of liquefaction and the reduction of horizontal subgrade reaction force, even though a bending moment equivalent to that generated in the piles in the case without improvement walls was generated. These experimental results show that the degree of liquefaction mitigation and the degree of decrease in horizontal subgrade reaction of the piles can be reasonably adjusted depending on the required

performance, based on the combination of appropriate separation and improved strength.

3.2 Depth distributions of various measured values in the experiments on CCPs

Figure 4 compares the depth distributions for the maximum values of various measurements obtained from the dynamic vibration test of the CCPs inside the ground improvement walls to those for the case without improvement walls.

Here, k_{hL}/k_{h0} values are compared to the data obtained for the points in the range from G.L. -1.0m to -6.0m, where k_{h0} values were clearly obtained.

It is understood that the shear strain in the ground was suppressed in all cases with improvement walls, but not in the case without improvement walls. The shorter was the separation and the higher was the improved strength in the calculated values for the range between G.L. -1.0m and -4.0m, the higher the suppression tended to be. Beyond that depth, we found no clear trend in separation or improved strength.

The values for excess pore water pressure are about the same for the cases with and without the improvement walls at some depths and are slightly suppressed for the cases with improvement wall at other depths. The values at G.L. -15.0m are exceptions. The bending moment tended to be considerably less in the 2*D* cases, in which the separation was the shortest, than in the case without measures. At G.L. -8.0m and G.L. -10.0m, the values for the 2*D* cases were significantly suppressed. The values for 3*D*-300 showed no clear difference from those in the case without the improvement walls.

The value of k_{hL}/k_{h0} in the range from G.L. -1.0m to -6.0m exceeded 1.0 for some depths, but the average value was lower than k_{h0}. The k_{hL} for the case without the improvement walls after vibration decreased to about 38% of the k_{h0} before vibration. The coefficient of horizontal subgrade reaction of the pile due to liquefaction was suppressed in 2*D*-300 by about 50%, which was 88% of the k_{h0} before vibration, in 3*D*-300 by about 20%, which was 58% of the k_{h0} before vibration, and in 2*D*-1000 by about 30%, which was 71% of the k_{h0} before vibration. Therefore, in these cases, it is not considered that taking actions that involve structural changes to the entire bridge system will be necessary. As with SPPs, it is considered that this improvement measure is an effective aseismic measure for bridges with CCP foundations, if appropriate conditions are set.

4 EFFECTS OF SEPARATION AND ENHANCED STRENGTH ON LIQUEFACTION MITIGATION

Figure 5 shows the relationship between the grid spacing for the ground improvement wall and the excess pore water pressure ratio ($\Delta u/\sigma_v$') based on experimental values for SPPs and CCPs. The grid spacing *L* was divided by the improvement depth *H* to give a generalized dimension ratio *L*/*H*. The value of $\Delta u/\sigma_v$' for each experimental case was obtained by averaging the values obtained between G.L. -1.0m and -10.0m, which were calculated for each measurement depth for excess pore water pressure in Fig. 3 and 4.

The results of the examination for volcanic ash ground in Figure 5(a) show that the suppression of $\Delta u/\sigma_v$' increases with decrease in separation. Furthermore, focusing on each value for the case with the separation 4*D* for SPPs and that with the 2*D* for CCPs, it is understood that $\Delta u/\sigma_v$' is suppressed at higher values of improved strength.

For comparison, the results in the Public Works Research Institute Joint Research Report (1999) on a similar study for sandy ground are shown in Figure 5(b). The liquefaction layer thickness in this current study (a) is 15.0m. The liquefaction layer thickness in the previous study on sandy ground (b) is 0.4m in the model vibration test and 10.0m in the centrifuge model test, and the area and volume enclosed by the ground improvement walls in (a) and (b) are different.

Figure 5(b) shows that there is a correlation between *L*/*H* and the suppression of $\Delta u/\sigma_v$' for sandy ground as well. However, it is understood from the figures that the extent of this suppression differs between volcanic ash ground (a) and sandy ground (b). The results of this study indicate that existing studies and standards for sandy ground cannot be applied directly to volcanic ash ground. This may be due to the presence of non-plastic fine particles as a characteristic of volcanic ash soils. Therefore, it is necessary to develop design techniques adapted to the liquefaction behavior of volcanic ash ground and pile foundation behavior in such ground.

Figure 5(a) plots $\Delta u/\sigma_v$' against *L*/*H*. Figure 6(a) plots $\Delta u/\sigma_v$' against *L*. Figure 6(b) shows the relationship between *L* and k_{hL}/k_{h0} obtained from the experiment.

The results of the study for sandy ground indicate that, based on the relationship shown in Figure 5(b), the ground improvement walls are effective in suppressing $\Delta u/\sigma_v$' in the range where *L*/*H* is less than about 0.8. If we apply *L*/*H*=0.8 to the centrifuge model test shown in Figure 5(b), then *L* corresponds to 8.0m. Although the degree of suppression differs from that in the sandy ground (Figure 6(a)), it is shown that even in volcanic ash ground, $\Delta u/\sigma_v$' inside the ground improvement walls is suppressed in the range where *L* is smaller than about 8.0m, regardless of the pile type. Figure 6(b) shows that k_{hL}/k_{h0} tends to be great when *L*

is less than about 7.0m, and when L is less than about 4.0m, the horizontal subgrade reaction coefficient exceeds 1.0 and is greater than that for the case without improvement.

Furthermore, it is assumed that the separation at which the grid-form ground improvement wall affects the existing pile depends on the actual distance, not on the ratio to the pile diameter. Therefore, Figure 7 shows L, based on the relationship in Figure 6(b), as the actual distance from the center of the outermost pile. The results show that k_{hL}/k_{h0} does not significantly exceed 1.0 at a separation larger than 2.0m from the center of the outermost pile.

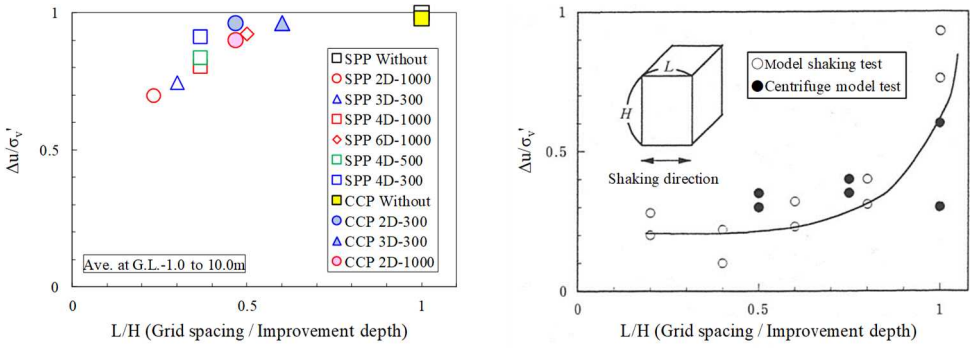

(a) Volcanic ash ground. (b) Sandy ground.

Figure 5. Dimension ratio L/H and Δu/σv' inside the ground improvement wall.

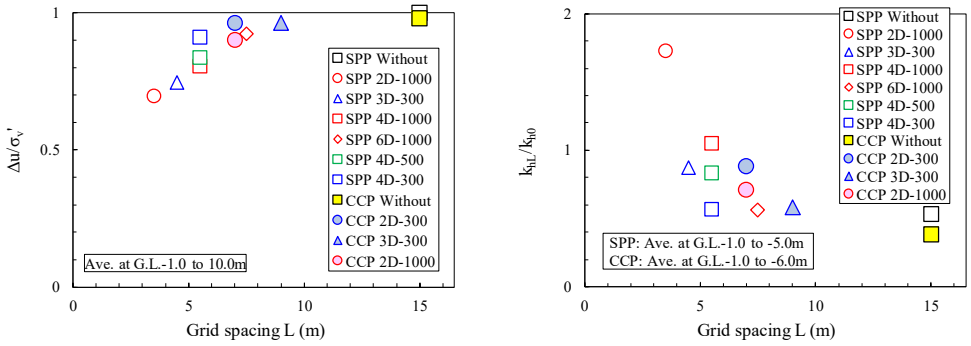

(a) $\Delta u/\sigma_v'$. (b) k_{hL}/k_{h0}.

Figure 6. Grid spacing L inside the improvement wall and $\Delta u/\sigma_v'$, k_{hL}/k_{h0}.

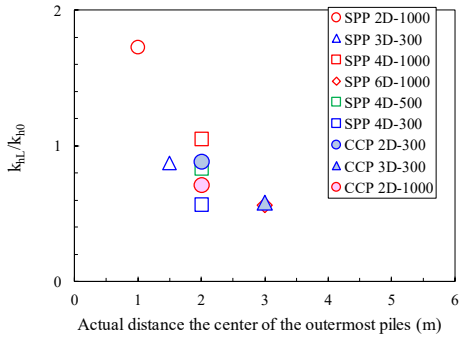

Figure 7. Relationship between actual distance and k_{hL}/k_{h0}.

5 CONCLUSIONS

This study investigated the applicability of a grid-form ground improvement technique, which involves surrounding the ground around pile foundations with a non-contact ground improvement wall, as a seismic reinforcement technique applicable when the stability of pile foundations is compromised solely by liquefaction in volcanic ash soil. The assessment was conducted through centrifuge model tests.

In this research, focusing on SPPs and CCPs commonly used as road bridge foundations, we examined how variations in the spacing from the outermost pile of the grid-form ground improvement wall and the improvement strength impact the effectiveness of liquefaction mitigation and their influence on existing piles.

As a result, it was found that, regardless of pile type and pile stiffness, the grid spacing should be less than 7.0m and the distance from the outermost pile center should be at least 2.0m to prevent a reduction in the coefficient of horizontal subgrade reaction due to liquefaction without affecting the existing bridge members or the entire bridge system. We concluded that the combination of the improvement walls and improved strength should be determined within this range depending on the required performance.

We are also considering the applicability of precast concrete piles with a diameter of 300mm and piles in sandy ground.

REFERENCES

Egawa, T., Yamanashi, T. and Isobe, K. (2018). Investigation on the aseismic performance of pile foundations in volcanic ash ground. *9th International Conference on Physical Modelling in Geotechnics*, pp. 879-884.

Soil Dynamics Laboratory et al., Research Center for Aseismic Technology, Public Works Research Institute, Ministry of Construction (1999). Design and Construction Manual of Countermeasures Against Liquefaction (Draft), *Joint Research Report of the Public Works Research Institute*, No. 186 (in Japanese).